Engineering Journal issn: 0125-8281

Article

Sappan Natural Dyed Biocomposites from Poly(Lactic Acid) and Aluminum Silicate Synthesized via Sol-Gel Method from Rice Husk Ash

Pajaera Patanathabutr[a,*] **and Nattakarn Hongsriphan**[b]

Department of Materials Science and Engineering, Faculty of Engineering and Industrial Technology, Silpakorn University, Nakhon Pathom, 73000, Thailand
E-mail: [a,*]Patanathabutr_P@su.ac.th (Corresponding author), [b]Hongsriphan_N@su.ac.th

Abstract. Precipitated silica synthesized via the sol-gel method from rice husk ash was used as the solid support for Sappan dye, extracted from natural Sappan heartwood. The precipitated silica was transformed into aluminium silicate in order to fix the natural dye onto the solid support for better high-temperature resistance during polymer melt compounding. The novel synthesized natural dye pigments were mixed into poly(lactic acid) (PLA) via the melt compounding using a pigment loading of 5 wt% and injection molded into specimens. Three types of compatibilizers as tetraethyl orthosilicate (TEOS), γ-glycidyloxypropyltrimethoxysilane (GPTMS) and γ-aminopropyltriethoxysilane (APTES) have been studied on the effect on different color shade and the improvement of compatibility by better interfacial adhesion between PLA and the pigments. Based on FTIR spectra, natural dye adsorption onto aluminium silicate was illustrated. It was found that the Sappan (red color) dyed pigments treated with GPTMS had the highest tensile modulus, while those treated with APTES provided the brightest color of the biocomposites. Thermal resistant of the biocomposites were improved when compared with pure PLA due to presence of silica.

Keywords: Poly(lactic acid); precipitated silica; Sappan natural dye; biocomposite.

ENGINEERING JOURNAL Volume 25 Issue 2
Received 7 February 2020
Accepted 25 November 2020
Published 28 February 2021
Online at https://engj.org/
DOI:10.4186/ej.2021.25.2.305

This article is based on the presentation at the International Conference on Engineering and Industrial Technology (ICEIT 2020) in Chonburi, Thailand, 11th-13th September 2020.

DOI:10.4186/ej.2021.25.2.305

1. Introduction

Poly(lactic acid) (PLA) are biodegradable polyesters derived from lactic acid, which can be obtained by bacterial fermentation from renewable materials by various microbial species, including bacteria, fungi, yeast, microalgae, and cyanobacteria. The reduction of lactic acid production cost has been widely researched [1, 2] in order to decrease cost of PLA production. Nowadays, PLA is industrially obtained through the polymerization of lactic acid or by the ring-opening polymerization of lactide (the cyclic dimer of lactic acid, as an intermediate) [3, 4]. Due to environmental concern about plastic waste, PLA has been encouraged to use as replacement of petroleum-based thermoplastics for short-life applications. In a composting environment, PLA waste can be hydrolyzed into smaller molecules (oligomers, dimers and monomers) and then degraded into CO_2 and H_2O by microorganisms in compost [5]. PLA can have properties ranging from amorphous glassy polymers with glass transition temperature of 60°C to semi-crystalline/highly crystalline polymers with crystalline melting points ranging from 130°C to 180°C. Quiescent nucleated crystalline products are essentially opaque, whereas stress-induced crystalline materials are transparent [4]. Optical properties of PLA are important in dyeing operations for textiles and in various packaging applications where clarity is desirable [6].

There have been various pigments adding into PLA in order to improve or adapt the final properties suitable for desired purpose, for example, adding calcium carbonate [7] into PLA could increase both tensile modulus and thermal stability, but adding microcrystalline cellulose [8] into PLA increased tensile modulus but reduced thermal stability. For aesthetics improvement, adding color is the interesting method to get attention from potential customers for any application. Pigments are usually added into plastics in order to give that particular plastics a unique appearance. Since bioplastics are being considered to replace non-biodegradable plastics, biobased pigments [9] that can give good aesthetics along with environmentally friendly is in demand. Pigments obtained from plants, animals, and insects have been used as food colorings and dyes, which the use of natural dyes in fabrics has been researched worldwide. Hussain *et al.* [10] reviewed the development in the dyeing of PLA textiles with disperse, vat, cationic and natural dyes. They summarized that dyeing with natural dyes would be a good eco-friendly alternative, however, it should be studied how to achieve brighter color with natural dyes with good fastness properties.

Caesalpinia sappan L. is a plant that belongs to the Leguminosae family, which these trees are distributed in Indonesia, Vietnam, Burma, India, South and Southwest China, and Thailand. The heart-wood of Sappan is commonly used for the extraction of red dye [11]. The major coloring component of Sappan heartwood is brazilin, however, brazilein which is the oxidized product of brazilin is also present [11, 12]. Their chemical structures are shown in Fig. 1. Under alkali condition, it will give intensely red color. Brazilin has been used to dye traditional textiles in many countries [13] including Thailand.

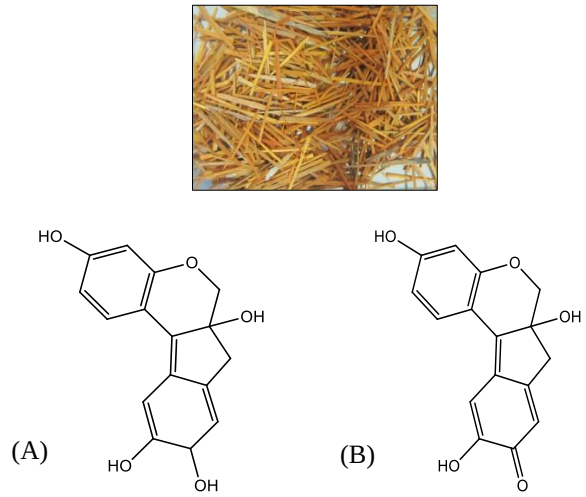

Fig. 1. Sappan heartwood and Sappan dye structures: (A) brazilin and (B) brazilein [12].

Lee *et al.* [14] prepared a nontoxic natural dye fabricated from an extract from *Caesalpinia sappan* L. (Sappan wood) using a micro-emulsion method. They found that the highest absorbance of color was obtained by using the aluminum mordant. Girdthep *et al.* [15] prepared a natural lake pigment of Sappan by converting the water-soluble Sappan dye to an insoluble pigment using kaolinite and alum via co-precipitation and adsorption under basic conditions. The composite films were prepared via a solution casting method using chloroform at room temperature. They reported that increasing the Sappan colorant-adsorbed kaolinite in the PLA composite films gave a darker pinkish-red color. They proposed that this type of composite film would be applied to produce the packaging film.

Since the conventional fabrication of thermoplastics into products is based on thermal processing, the adsorbent for Sappan dye should be an inorganic pigment that can adsorb the water-soluble Sappan dye well and acts as thermal protector for natural dye during the melt processing of PLA (180-200°C). Therefore, this study synthesized the precipitated silica from rich husk ash via the sol-gel method, and then transformed them into aluminium silicate in order to become a suitable mordant for natural dye fixation. These aluminium silicate was natural dyed directly by an aqueous extract from Sappan heartwood. Then, PLA and the Sappan dyed aluminium silicate were melt compounded in a twin-screw extruder and fabricated into specimens by an injection molding machine. Three types of silane coupling agents as compatibilizers; tetraethylorthosilicate (TEOS), γ-glycidyloxypropyltrimethoxysilane (GPTMS), and γ-aminopropyltriethoxy silane (APTES), were studied to improve compatibility between PLA and Sappan dyed aluminium silicate. Color, mechanical, and

thermal properties of the biocomposites were evaluated and compared with pure PLA.

2. Experimental

2.1. Materials

Poly(lactic acid) (PLA3001D) was purchased from NatureWorks LLC, USA, which had a density of 1.24 g/cm^3 and melt flow index (MFI) of 7 g/10 min (at 210°C, 2.16 kg). Rice husk ash was kindly provided from a local clay brick factory that used Thai rice hush as its biomass energy. Wood pieces from heartwood of *Caesalpinia sappan* L. was kindly provided by a local wood supplier. Aluminium sulphate monohydrate ($Al_2(SO_4)_3.18H_2O$), citric acid monohydrate, and sodium hydroxide were purchased from RCI Labscan Ltd. Tetraethyl orthosilicate (TEOS) was purchased from Fluka, Honeywell International Inc., USA. Three types of silane coupling agents as compatibilizers; γ-glycidyloxypropyltrimethoxy silane (GPTMS) and γ-aminopropyltriethoxy silane (APTES) were purchased from Sigma-Aldrich Co LLC, Germany. All chemicals had the purity more than 98% and used as received. The chemical structures of TEOS, GPTMS, and APTES are presented in Fig. 2.

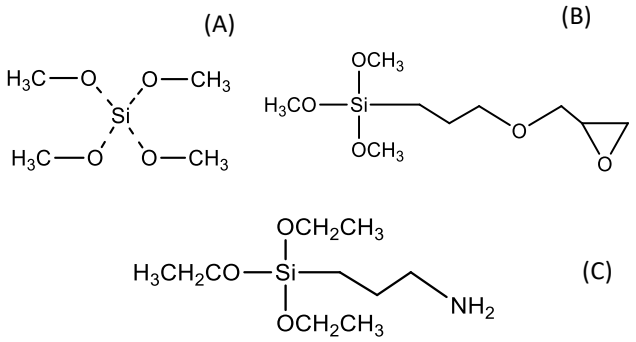

Fig. 2. Chemical structures of TEOS (A), GPTMS (B), and APTES (C).

2.2. Synthesis of Precipitated Silica from Rice Husk Ash by the Sol-Gel Method

Twenty grams of Thai rice husk ash from a local clay brick factory were dissolved in a round bottom flask containing 600 ml of 1M NaOH solution at 120°C and boiled with reflux for 12 hours. Then, the solution was filtered undissolved portion using fine cheesecloth. The filtrate of sodium silicate solution of 500 ml was placed in a 1000 ml beaker, and 1M citric acid was dropped into the solution until solution pH was adjusted to 7. Then, neutralized solution was stirred continuously 12 hours for the complete precipitation of silica. Then, the precipitated silica was filtered out and washed with distilled water until reaching pH 7. Precipitated silica was dried in an air-circulating oven at 80°C for 24 hours.

2.3. Preparation of Aluminium Silicate from Precipitated Silica

The precipitated silica was ball milled and sieved using a sieve shaker (120-325 mesh). Then, twenty grams of sieved precipitated silica was dispersed in a round bottom flask containing aluminium sulphate of 115.46 gram in distilled water of 1,000 ml. The pH of suspension was adjusted to 4 by Citric acid. Suspension was stirred and refluxed at 100°C for 1 hour. The obtained aluminium silicate particles were filtered out and washed with distilled water until reaching pH 7. Aluminium silicate particles were dried in an air-circulating oven at 80°C for 48 hours.

2.4. Fixing Natural Dye from *Caesalpinia sappan* L. onto Aluminium Silicate Surface

Natural dye was prepared by streaming heartwood pieces of *Caesalpinia sappan* L. 60 grams for 1 hour, boiled, and refluxed in distilled water of 600 ml at 100°C for 12 hours, and then hot filtered using filter paper to obtain Sappan dye solution. Twenty grams of aluminium silicate particles were suspended in the Sappan dye solution of 200 ml, boiled and refluxed at 100°C for 1 hour. Then, dyed aluminium silicate particles were filtered out and dried in an air-circulating oven at 80°C for 48 hours. Figure 3 shows Sappan dyed aluminium silicate compared with the original aluminium silicate. It is seen that the red color extracted from the Sappan heartwood were fixed onto the aluminium silicate particles.

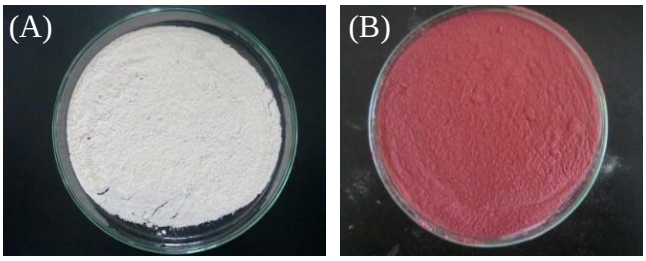

Fig. 3. Aluminium silicate (A) and Sappan dyed aluminium silicate (B).

2.5. Pigment Treatment by Compatibilizers

Three types of compatibilizer, TEOS, GPTMS, and APTES were used to treat dyed aluminium silicate. All of them were in liquid form. The content of compatibilizer used was 3 or 6 wt% of composite weight. The compatibilizer was dissolved in a solution of water/ethanol and then sprayed directly to the Sappan dyed aluminium silicate particles. Treated pigments were dried thoroughly in an air-circulating oven at 120°C for 24 hours.

2.6. Compounding and Fabrication of Pure PLA and PLA/Aluminium Silicate Biocomposites

Before compounding, PLA pellets were dried in an air-circulating oven at 40°C for 12 hours. PLA pellets and dried aluminium silicate (or Sappan dyed aluminium silicate) particles were compounded with the fixed pigment loading of 5 wt% biocomposites. The compounding was carried out in a co-rotating twin-screw extruder (SHJ-25, Yongteng, China) with a screw speed of 120 rpm and a barrel/die temperature profile between 140 to 180°C. Extrudates were water cooled, pelletized, and dried immediately in an air-circulating oven at 60°C for 12 hours. Dogbone-shape and Izod impact specimens were fabricated by an injection molding machine (Battenfeld, BA250CDC, England) using the barrel/nozzle temperature of 160/180°C and the mold temperature of 30°C. PLA pellets was also extruded and fabricated under the same thermal history, which was designated as pure PLA samples.

2.7. Characterization and Testing

Composition of rice hush ash was characterized by a wavelength dispersive X-ray fluorescence spectrometer (XRF, Axios PW4400, MalvernPanalytical, England) which the tests were performed under oxygen and non-oxygen condition. Precipitated silica, aluminium silicate, and Sappan dyed aluminium silicate were also characterized by a FT-IR spectrometer, (Vertex 70, Bruker, USA), which the spectra were recorded between 4000 and 400 cm^{-1}. Samples were placed on the ATR attachment and a minimum of 32 scans were averaged with a resolution of 2 cm^{-1} within the 4000-400 cm^{-1} range.

Thermal property study was evaluated using a differential scanning calorimeter (Pyris 1, Perkin Elmer, USA). Samples of 5-10 mg were tested in a heat-cool-heat mode and heated from 25 to 200°C at a heating rate of 5°C/min under nitrogen atmosphere. Glass transition temperature (T_g), cold crystallization temperatures (T_{cc}), and crystal melting temperatures (T_m) were determined from thermogram and reported. The percentage crystallinity (X_c) was calculated as the following equation:

$$\%X_c = \frac{\Delta H_m}{\Delta H_m^o} \times \frac{100}{w} \quad (1)$$

where w was weight fraction of PLA in the composite, ΔH_m was melting enthalpy of sample (J/g), and ΔH°_m was melting enthalpy of 100% crystalline PLA (93.0 J/g) [16].

Thermal stability of biocomposites was characterized by a thermo-gravimetric analyzer (TGA7 HT, Perkin Elmer, USA). Samples were heated from 50 to 600°C at a heating rate of 10°C/min under nitrogen atmosphere. Onset degradation temperatures, peak degradation temperatures (T_m) and char residue were determined from thermogram and reported.

Color of injection molded specimen was evaluated in CIE color space system. CIE L*a*b* of specimens were measured using a color reader (CR-10, Konica Minolta, Japan). Five samples were measured L*a*b* values under a control light environment and calculated the average values.

Tensile testing was carried out in accordance to ASTM-D638 using a universal testing machine (LR 50K, Lloyd Instrument, England). The test was done using a crosshead speed of 50.8 mm/min. Eight specimens were tested, which the average and the standard deviation of tensile modulus, ultimate tensile strength, and elongation at break were calculated.

Notched Izod impact testing was carried out in accordance to ASTM-D256 using an impact tester (Zwick, B5102.202, Germany) with a pendulum hammer of 4.0 Joule. Ten specimens were tested, which the average and the standard deviation of impact strength were calculated.

Morphology of fracture surface specimens after tensile test was examined using a scanning electron microscope (SEM, Cam Scan MX-2000, England). The fractured surface was gold coated prior to inspection to avoid electrostatic charging before examination.

3. Results and Discussion

3.1. Characterization of Sappan Dyed Aluminium Silicate

Prior to synthesis of precipitated silica via the sol-gel method, the composition of Thai rice husk ash were determined using the XRF analysis. The test results under oxygen and non-oxygen conditions are presented in Table 1 and Table 2, respectively. Thai rice husk ash consists of silicon (Si) about 86.2%, mostly in the form of silicon oxide (SiO_2). There is small amount of potassium oxide (K_2O), calcium oxide (CaO), ferrous oxide (Fe_2O_3), and manganese oxide (MnO). The chemical compositions are similar to those reported by Deng *et al.*[17]and Mor et al.[18]. However, it should be noted that the received rice husk ash does not show any trace of alumina (Al_2O_3).

The precipitated silica, prepared aluminium silicate, and Sappan dyed aluminium silicate were characterized by FTIR analysis and compared as shown in Fig. 4. The characteristics FTIR of Brazilin and Brazilein was not reported which were studied and reports in details by Oliveira *et al.* [19]. For the precipitated silica (Fig. 4A), the broad strong absorption peak at 3455 cm^{-1} is attributed to the asymmetrical stretching vibration of the single bond -OH groups [20], which are from the free water and bound water on the silica particles. The strong absorption peak at 1591 cm^{-1} is also assigned to the bending vibration of H-O-H derived from the pore water and surface absorbed water. The strong absorption peak at 1103 cm^{-1} is the characteristic peak assigned to the asymmetric stretching of Si-O-Si bonds [21]. The broad absorption band around 800-900 cm^{-1} is attributed to symmetric stretching of Si-O-Si bonds and Si-OH bonds [20, 21], and the peak at 467 cm^{-1} is assigned to the rocking bond of the Si–O bond [22].

Table 1. Compositions of Thai rice husk ash from XRF (Oxygen).

Composition	SiO_2	K_2O	CaO	TiO_2	MnO
Value, wt%	94.8	2.95	1.52	0.029	0.126
Composition	Fe_2O_3	CuO	ZnO	BrO	
Value, wt%	0.463	0.023	0.0420	0.0042	

Table 2. Mineral content of Thai rice husk ash from XRF (Non-oxygen).

Minerals	Si	K	Ca	Ti	Mn
Value, wt%	86.20	8.08	3.84	0.064	0.365
Minerals	Fe	Cu	Zn	Br	
Value, wt%	1.22	0.072	0.131	0.017	

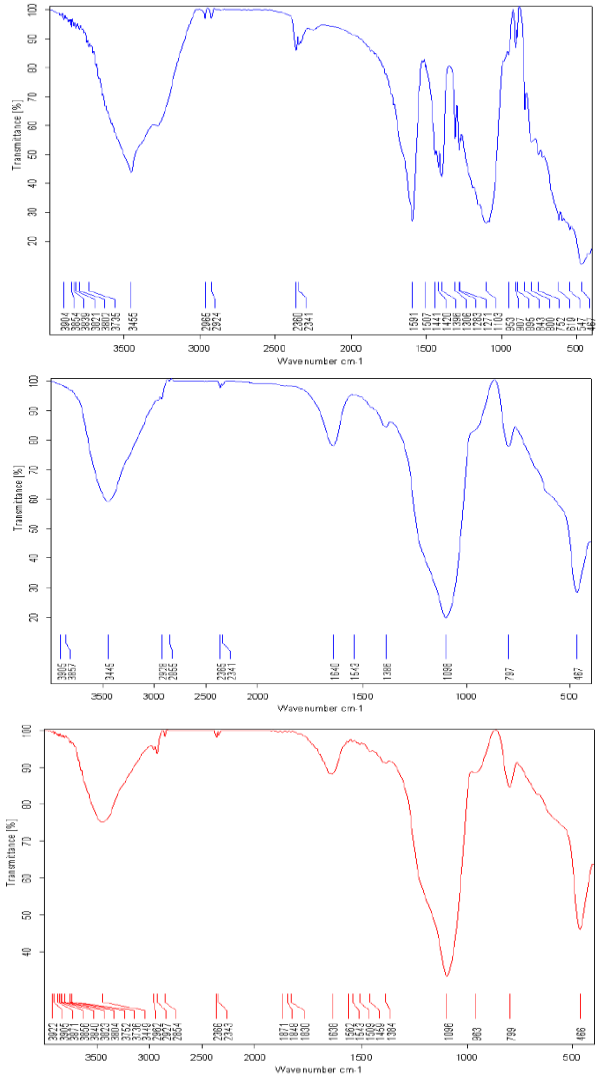

Fig. 4. FTIR spectra of precipitated silica (A), prepared aluminium silicate (B), and Sappan dyed aluminium silicate (C).

For prepared aluminium silicate (Fig. 4B), the broad spectrum at 3445 cm^{-1} is assigned to the O–H stretching peak of water residues [23] and the wavenumber at 1098 cm^{-1} is assigned to Si-O-Si stretching, which is shifted to lower wavenumber implying interaction between silica and aluminium ions. Moreover, the absorption peak at 1591 cm^{-1} is absent indicating that the bound water are removed because of electrostatic interaction between aluminium ion and silica. The wavenumber at 1640 cm^{-1} is attributed to Si-O-Al stretching [24] and at 797 cm^{-1} is attributed to Si-O-Al from interaction between silica and aluminium ion (Al^{3+}). The wavenumber at 467 cm^{-1} is assigned to the rocking bond of the Si–O bond.

For Sappan dyed aluminium silicate (Fig. 4C), the similar IR pattern is similar to the spectra of aluminium silicate. The wave number at 3449 cm^{-1} is assigned to the O–H stretching peak of water residues and the wavenumber at 1096 cm^{-1} is assigned as Si-O-Si. The wavenumber at 799 cm^{-1} is attributed to Si-O-Al, which is shifted a little from the metal chelate between aluminium silicate and Sappan dye. The wavenumber at 466 cm^{-1} is assigned to the rocking bond of the Si–O bond.

According to Donosea *et al.* [25], $Al(OH)^{2+}$ is expected to be the most dominate species present in solution at pH equal to 4 because citric acid is used to justify pH. Since the surface of silica is negative charge in the water, $Al(OH)^{2+}$ ions could be static adsorbed on silica surface which they change to be Al^{3+} ions after drying in oven. Figure 5 illustrates the static adsorption of Al^{3+} ions onto the silica (SiO_2) surface when aluminium silicate is suspended in the Sappan dyed solution. The interaction between Sappan dye and aluminium silicate is proposed that the chelate linkage between hydroxyl groups of the organic dye and aluminium ions is formed as illustrated in Fig. 6. As a result of this binding, aluminium silicate becomes the solid support for Sappan dye (brazillin) presenting the red color particles.

$$Al^{3+} + H_2O \rightarrow Al(OH)^{2+} + H^+$$

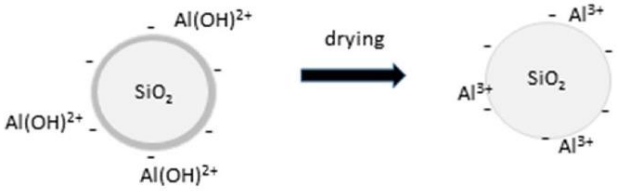

Fig. 5. Illustration shows static adsorption of aluminium ions on silica surface.

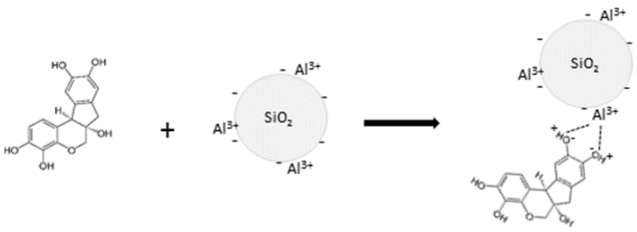

Fig. 6. Illustration shows brazillin adsorption on silica surface via aluminium mordant.

3.2. Characterization of Pure PLA and Sappan Dyed Biocomposites by DSC

In order to characterize performance of different compatibilizers, thermal properties of the Sappan dyed biocomposites were studied by DSC and compared with pure PLA. All biocomposites showed the similar pattern of thermal properties of pure PLA, although the crystal melting temperatures became the double peak in the 2nd heating scan compared to the single peak in the 1st heating scan. There was no crystallization temperature (T_c) present in the cooling scan in all samples indicating these Sappan dyed aluminium silicate particles could not act as nucleating agent for PLA molecules.

From the 2nd heating scan, the glass transition temperatures (T_g), the cold crystallization temperatures (T_{cc}), and the crystal melting temperatures (T_m) of pure PLA and biocomposites adding Sappan dyed aluminium silicate treated with TEOS, GPTMS, and APTES are summarized in Table 3. It was found that $T_{g,PLA}$ of pure PLA was 59.3°C, while those $T_{g,PLA}$ of biocomposites were shifted to occur at slightly higher temperature. This observation was similar to the study by Dorigato *et al.*[26] that the presence of silica nanoparticles slightly increased $T_{g,PLA}$ and the study by Abdulkhani *et al.*[27]that adding cellulose nanofiber (CNF) into PLA could increase $T_{g,PLA}$. This shift of $T_{g,PLA}$ indicated the interaction between PLA molecules and these silane-treated aluminium silicate particles, however, the shift of $T_{g,PLA}$ did not differentiate among the biocomposites treated by different types at different concentration (3 wt% and 6 wt%) of compatibilizers in this study. Compared to pure PLA, the biocomposites showed higher T_{cc} implying these dyed aluminium silicate particles inhibited the recrystallization of PLA molecules. This was in contrast with the work by Ortenzi *et al.*[28] that they found the presence of silica nanoparticles modified with silanes greatly enhanced crystallinity of PLA, which evidenced by the appearance of exothermic crystallization during the cooling step and the reduction of T_{cc} in the 2nd heating step. This could be attributed to the dispersion of Sappan dyed aluminium silicate particles in micro-scale, and thus these micro-sized particles restricted the PLA molecules, having rigid segments to crystallize. The study on the effect of Sappan dye and its concentration will be further studied.

Beltrán *et al.* [29] reported the double melting peak of PLA around 150°C attributed to the melt re-crystallization mechanism, which the less perfect crystals melted at lower temperatures, reorganized in more stable crystals during the heating, and then melted at higher temperatures. For the heating rate used in this work, the recrystallization process in pure PLA occurred significantly to obtain high $X_{c,2}$ as a result. Nevertheless, this process was suppressed by the Sappan dyed aluminium silicate particles reducing $X_{c,2}$, especially in the APTES treated biocomposites. Compared among the biocomposites, the GPTMS 3 wt% treated biocomposites had the highest X_c which was closed to that of pure PLA. This might be used to indicate that the best dispersion of Sappan dyed aluminium silicate particles occurred in the composited that these pigments were treated with GPTMS 3 wt%.

Table 3. Glass transition temperatures (T_g), cold crystallization temperatures (T_{cc}), crystal melting temperatures (T_m), and degree of crystallinity (X_c) of pure PLA and biocomposites adding Sappan dyed aluminium silicate from the 2nd heating scan.

Sample	T_g (°C)	T_{cc} (°C)	T_m (°C)		ΔH_m(J/g)		X_c (%)	
			$T_{m,1}$	$T_{m,2}$	$\Delta H_{m,1}$	$\Delta H_{m,1}$	$X_{c,1}$	$X_{c,2}$
Pure PLA	59.3	107.6	148.3	155.5	5.260	8.724	3.896	6.462
TEOS 3 wt%	60.2	106.8	148.7	156.4	5.811	6.749	4.304	4.999
TEOS 6 wt%	60.8	108.9	150.1	157.6	5.545	6.970	4.107	5.163
GPTMS 3 wt%	60.4	110.5	149.7	156.4	7.816	6.475	5.790	4.796
GPTMS 6 wt%	60.5	113.5	150.4	156.4	8.112	1.566	6.009	1.160
APTES 3 wt%	59.4	115.3	150.7	155.8	10.192	1.305	7.549	0.966
APTES 6 wt%	60.1	114.7	150.6	156.2	6.899	2.320	5.110	1.718

3.3. Characterization of Pure PLA and Sappan Dyed Biocomposites by TGA

Figure 7 shows TGA thermograms of pure PLA and biocomposites adding treated Sappan dyed aluminium silicate, which Table 4 summaries degradation temperatures (T_d) and residue percentage. It was seen that adding treated pigments reduced the T_d of PLA matrix

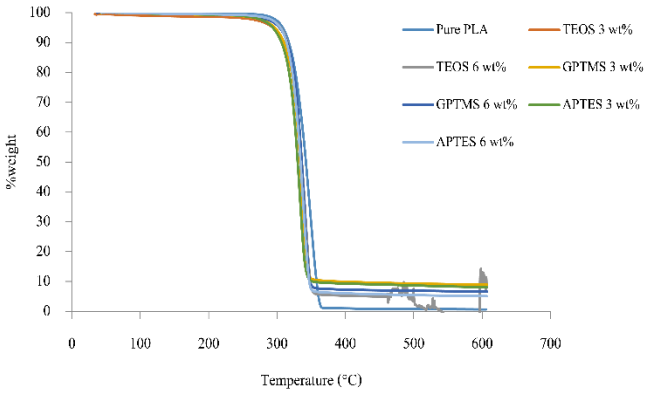

Fig. 7. TGA thermograms of pure PLA and bio-composites adding Sappan dyed aluminium silicate treated with TEOS, GPTMS, or APTES.

compared to pure PLA that had experienced the same thermal history. Since these compatibilizers were small organic molecules, they degraded at a relatively lower temperature and then initiated the thermal degradation of PLA molecules. However, the char residue after thermal degradation of the biocomposites was higher than the fixed number of pigment loading at 5 wt%. This would imply that aluminium silicate particles absorbed free radicals during the degradation and thus phenolic

compounds from the Sappan dyes could transform into char residues of carbonaceous compounds.

Table 4. Degradation temperatures (T_d) of pure PLA and PLA-based biocomposites adding dyed aluminium silicate treated with TEOS, GPTMS, or APTES.

Sample	Onset T_d (°C)	End T_d (°C)	Inflection point or T_d (°C)	% Char residue
Pure PLA	272.7	375.7	349.7	1.09
TEOS 3 wt%	249.2	364.3	338.0	9.71
TEOS 6 wt%	256.1	368.6	341.9	5.53
GPTMS 3 wt%	255.2	359.1	337.4	10.44
GPTMS 6 wt%	258.7	360.0	340.0	7.67
APTES 3 wt%	247.0	362.6	333.0	9.67
APTES 6 wt%	269.3	368.6	339.9	6.33

3.4. Color Measurement of Pure PLA and Sappan Dyed Biocomposites

According to Dong-Kyu Lee *et al.* [14], Sappan wood was a multicolored material containing yellow and red components which the most suitable mordant for the dye fixation was aluminium (Al). Figure 8 shows color of pelletized pure PLA and composite compounds between PLA and Sappan dyed aluminium silicate treated with TEOS, GPTMS, or APTES. The color of the pure PLA pellets after extruded is translucent. The color of composite pellets adding Sappan dyed aluminium silicate treated with TEOS and GPTMS is brownish red/orange while it is pinkish red for pellets adding Sappan dyed aluminium silicate treated with APTES. Since the fixation of Sappan dye with aluminium silicate was the same, the difference of the color shading resulted from the acidic/basic nature of the compatibilizers used in this study. Madhu *et al.* [30] reported that the color extraction from Sappan wood was bright yellow color ($\lambda_{max,UV/VIS}$ = 443 nm) in acidic pH and carmine red color ($\lambda_{max,UV/VIS}$= 537 nm) in alkaline pH. For treating Sappan dyed aluminium silicate with APTES, the cationic amino groups could form ionic bonding with the anionic charge from the phenolic compounds in Sappan dye [12]. This interaction caused the π-π^* transition to be weaker so that the UV/VIS absorption was toward the longer wavelength (red color). On the other hand, the neutral TEOS and weak acidic GPTMS could form the dipole-dipole interaction with the phenolic compounds in Sappan dye, so that the UV/VIS absorption was in the shorter wavelength (yellow color).

It is well known that natural dye is sensitive to heat and light. Adsorption Sappan dye onto aluminium silicate could allow the dye to withstand higher temperature due to the high heat capacity of the ceramic particles. This could allow the melt processing of the biocomposites adding natural dye. Figure 9 shows pure PLA and Sappan dyed composite specimens that had experienced two-time thermal processing; including compounding in a twin-screw extruder at 180°C and injection molding at 180°C.

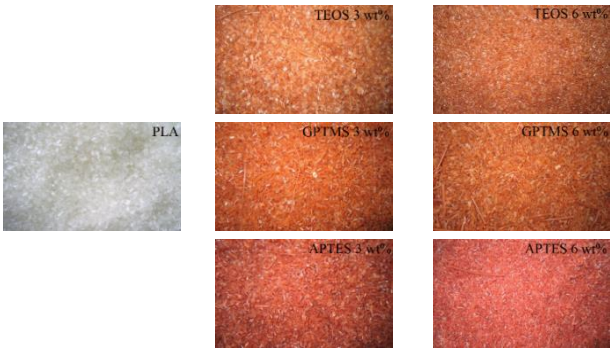

Fig. 8. Color of pure PLA pellets (extruded) and Sappan dyed composite pellets (extruded) treated with TEOS, GPTMS, or APTES.

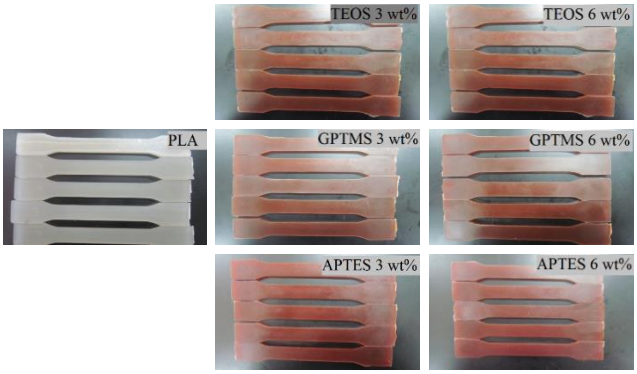

Fig. 9. Color of pure PLA and PLA-based biocomposites adding dyed aluminium silicate treated with TEOS, GPTMS, or APTES after injection molding.

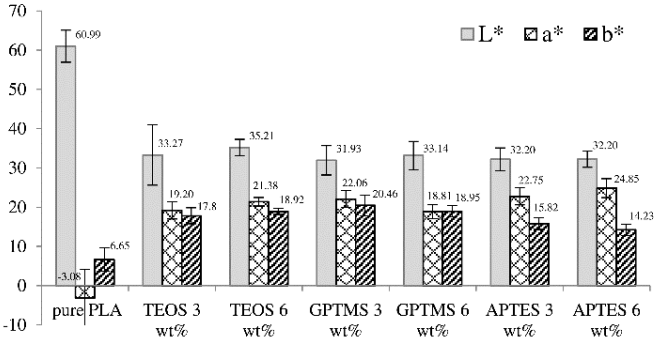

Fig. 10. L*a*b* measurement of pure PLA and Sappan dyed biocomposites treated with TEOS, GPTMS, or APTES.

It was observed that the color of the Sappan dyed biocomposites treated with TEOS or GPTMS was yellowish red, and it was dark red when treated with APTES. The color measurement was measured by a color reader, which the L*a*b are presented in Fig. 10. It was found that adding Sappan dyed aluminium silicate reduced the lightness (L) of the pure PLA from 61 to 32-35, since the opaque aluminium silicate particles were distributed in the PLA matrix. From CIELAB color space, the a axis extends from green (-a) to red (+a) and the b axis from

blue (-b) to yellow (+b). By this interpretation, the pure PLA had the b value indicating yellowness of the specimens after the melt processing. According to Al-Itry *et al.*[31], they proposed that the thermal degradation mechanism of PLA was hydrolysis and random main-chain scission (a β-C-H hydrogen transfer reaction) leading to a vinyl ester and acid end groups, which these vinyl esters would polymerize and then thermally degrade into yellow or brown polyenes.

Comparison between the biocomposites adding Sappan dyed aluminium silicate, the biocomposites treated with APTES had the highest +a value (red) but the lowest +b value (yellow) corresponding to dark red color as seen by naked eyes. On the other hand, the biocomposites treated with TEOS and GPTMS had the +a value in the closed number with the +b value (yellow) of 17-20 that caused these specimens were seen yellowish red.

3.5. Tensile Properties of Pure PLA and Sappan Dyed Biocomposites

Figure 11 shows tensile modulus of pure PLA and biocomposites between PLA and Sappan dyed aluminium silicate particles treated with three types of compatibilizers. It was found that the surface treated aluminum silicate particles increased the rigidity of the PLA-based biocomposites. As the pigment loading in all biocomposites was fixed at 5 wt%, it was clearly observed that GPTMS was the most efficient compatibilizer to improve interfacial adhesion between PLA matrix and aluminium silicate particles. This result correlates with the DSC test that the biocomposites treated with 3 wt% GPTMS had the highest total X_c of PLA. However, there was no significant difference in tensile modulus between GPTMS 3 wt% and 6 wt% treated biocomposites.

Figure 12 shows tensile strength and elongation at break of pure PLA and biocomposites with various compatibilizers. It is seen that tensile strength of PLA biocomposites was in the same range which were lower than that of pure PLA. Elongation at break of Sappan dyed PLA biocomposites treated with all types of compatibilizers, was reduced from 5 % to be around 2 % compared to pure PLA. This was due to adding aluminium silicate particles which are particulate shape, would ease the crack propagation of brittle PLA matrix under tension load.

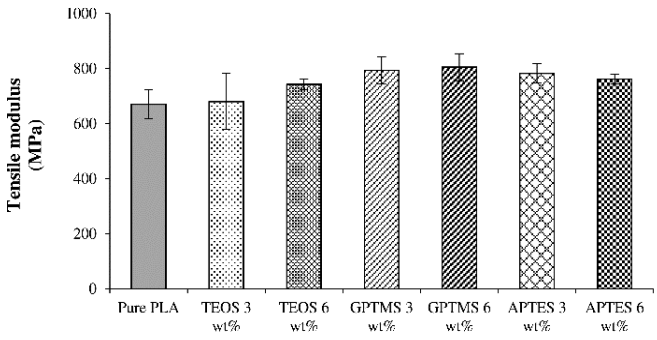

Fig. 11. Tensile modulus of pure PLA and PLA-based biocomposites adding dyed aluminium silicate treated with TEOS, GPTMS, or APTES.

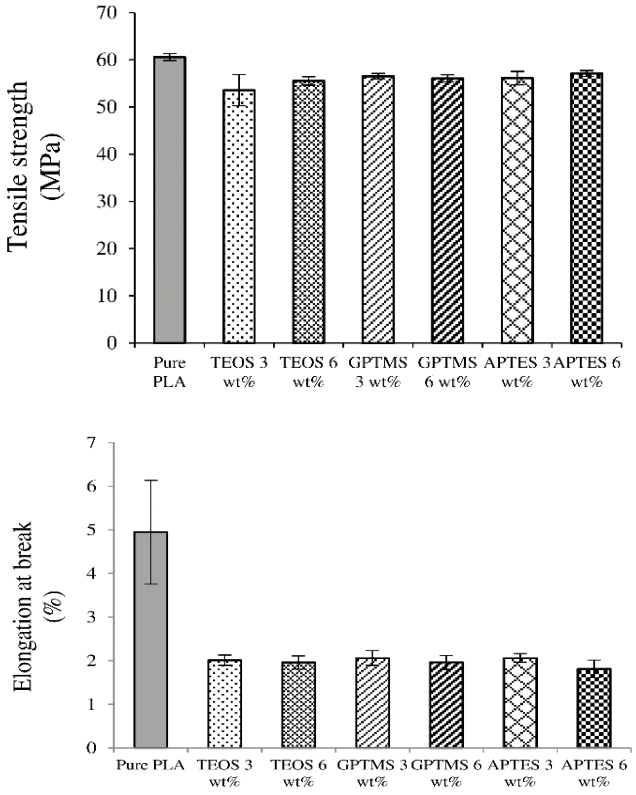

Fig. 12. Tensile strength and elongation at break of pure PLA and PLA-based biocomposites adding Sappan dyed aluminium silicate treated with TEOS, GPTMS, or APTES.

3.6. Impact Properties of Pure PLA and Sappan Dyed Biocomposites

Toughness of the Sappan dyed biocomposites is evaluated and compared with pure PLA in term of notched Izod impact strength as shown in Fig. 13. It is observed that using TEOS of 3 wt% was not sufficient enough to provide suitable interfacial adhesion between PLA matrix and aluminium silicate particles as TEOS has no functional group to react chemically with PLA while GPTMS and APTES have. When these pigments were treated with GPTMS or APTES at silane concentration of 3 wt% would help to provide fair adhesion between PLA matrix and the particulate pigments during the impact loading.

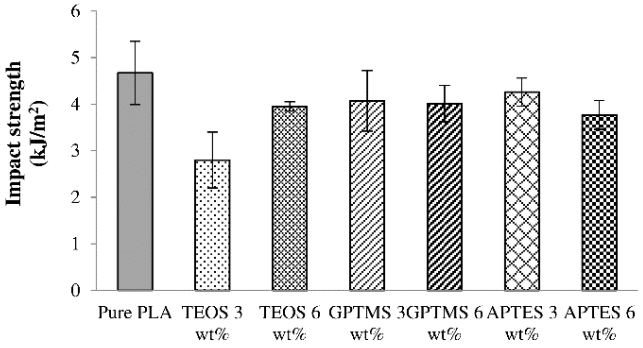

Fig. 13. Notched Izod impact strength of pure PLA and PLA-based biocomposites adding dyed aluminium silicate treated with TEOS, GPTMS, or APTES.

3.7. Morphology of Pure and Sappan Dyed Bio-Composites

Figure 14 shows SEM micrographs of fractured surface of pure PLA and its biocomposites with 5 wt% Sappan dyed aluminium silicate treated with different types of compatibilizers. It was found that the failure of the biocomposites was shifted toward higher brittleness compared to the pure PLA specimens. Pure PLA showed localized ductile as broad strips occurs during the impact failure. However, adding Sappan dyed aluminium silicate into the PLA matrix, the long broad strips disappeared while the crack propagation line at the interface of the matrix and the pigments was present due to silane coupling agents can improve the connection between the dispersed phases of pigments and the matrix. This indicates that dyed aluminium silicate became stress concentrators that impact energy initiated crack around the dispersed phases and then propagated through these pigment particles for specimen failure.

Figure 15 shows SEM micrographs at 2000X magnifications which revealed the interfacial adhesion between PLA matrix and Sappan dyed aluminium silicate that was treated with TEOS, GPTMS, and APTES. It is seen that the pigment particles were embedded inside the PLA matrix and some fine filaments due to deformation of silane coupling treated on Sappan dyed aluminium silicate in the PLA matrix. Thus, it showed the better adhesion between the PLA matrix and dispersed phases of pigment particles. This confirms good load transfer between phases during the elastic response prompting the biocomposites to show higher tensile modulus.

4. Conclusion

Precipitated silica was synthesized and transformed into aluminium silicate, and then successfully dyed with the Sappan dye extracted from Sappan heartwood. These natural dyed particles could be used as the red color pigment that was able to be melt-compounded with PLA and injection molded into specimens. Three types of compatibilizers; TEOS, GPTMS, and APTES, were used to improve interfacial adhesion between PLA matrix and Sappan dyed aluminium silicate particles. SEM micrographs showed that these treated particles were embedded and dispersed well in the PLA matrix. The biocomposites treated with GPTMS gave the highest tensile modulus as a silane coupling agent acts as a compatibilizer to improve adhesion between the matrix and the pigments. However, tensile strength and impact strength of the biocomposites were reduced marginally due to stress concentration of the particulate micro-scale pigments. SEM micrographs shows that these dispersed phases initiated crack around them and propagated resulting brittleness inside the materials. The Sappan dyed biocomposites after injection molding showed different color shade as brownish red when treated with TEOS or GPTMS, and was dark red when treated with APTES. The difference of color shade was due to the acidic/basic nature of the compatibilizers used.

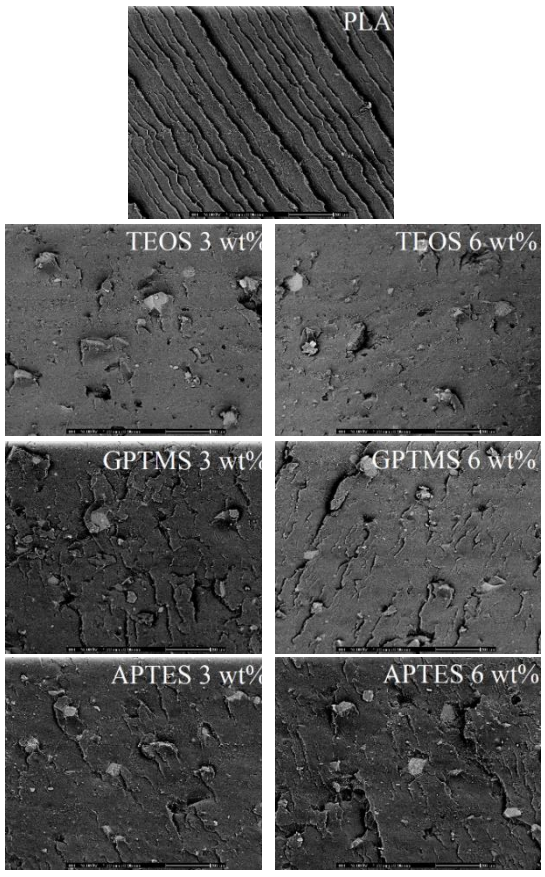

Fig. 14. SEM micrographs (magnification of 100X) revealed impact fracture surface of pure PLA and PLA-based biocomposites adding dyed aluminium silicate treated with TEOS, GPTMS, or APTES.

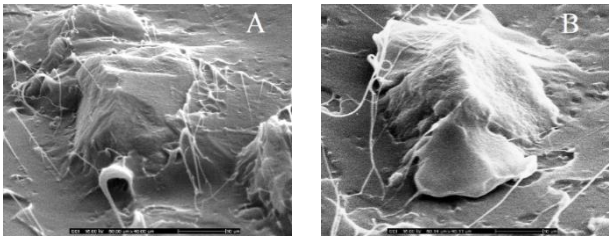

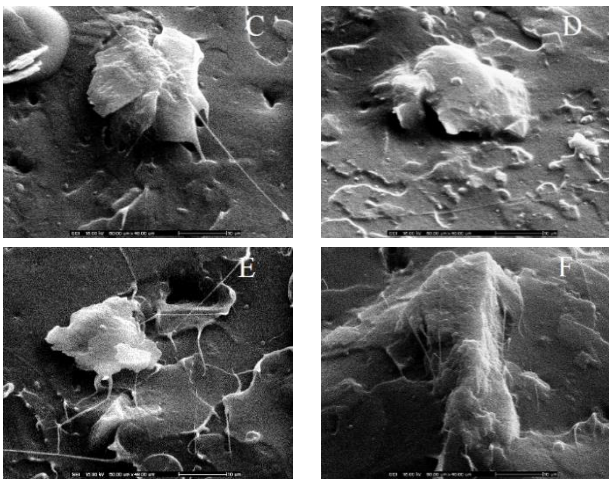

Fig. 15. SEM micrographs (magnification of 2000X) revealed interfacial adhesion between PLA matrix and dyed aluminium silicate treating with (A) TEOS 3 wt%, (B) TEOS 6 wt%, (C) GPTMS 3 wt%, (D) GPTMS 6 wt%, (E) APTES 3 wt%, and (F) APTES 6 wt%.

Acknowledgement

The authors would like to thank the Department of Materials Science and Engineering, Faculty of Engineering and Industrial Technology, Silpakorn University for funding and instrument support throughout the research. The authors also would like to appreciate the research works performed by Miss Kamonwan Soonthornsart, Miss Prangsiri Maneenoun, and Miss Wannapon Pinduangour, under the authors' supervision.

References

[1] M. A. Abdel-Rahmanab, Y. Tashirocd, and K. Sonomotoa, "Recent advances in lactic acid production by microbial fermentation processes," *Biotechnology Advances*, vol. 31, no. 6, pp. 877-902, 2013.

[2] B. K. Ahring, J. J. Traverso, N. Murali, and K. Srinivas, "Continuous fermentation of clarified corn stover hydrolysate for the production of lactic acid at high yield and productivity," *Biochemical Engineering Journal*, vol. 109, no. pp. 162-169, 2016.

[3] M. Murariu and P. Dubois, "PLA biocomposites: From production to properties," *Advanced Drug Delivery Reviews*, vol. 107, no. pp. 17-46, 2016.

[4] J. Lunt, "Large-scale production, properties and commercial applications of polylactic acid polymers," *Polymer Degradation and Stability*, vol. 59, no. 1-3, pp. 145-152, 1998.

[5] Y. Tokiwa and B. P. Calabia, "Biodegradability and biodegradation of poly(lactide)," *Applied Microbiology and Biotechnology*, vol. 72, no. 2, pp. 244-251, 2006.

[6] S. Farah, D. G. Anderson, and R. Langer, "Physical and mechanical properties of PLA, and their functions in widespread applications — A comprehensive review," *Advanced Drug Delivery Reviews*, vol. 107, no. pp. 367-392, 2016.

[7] K. Piekarska, E. Piorkowska, and J. Bojda, "The influence of matrix crystallinity, pigment grain size and modification on properties of PLA/calcium carbonate biocomposites," *Polymer Testing*, vol. 62, pp. 203-209, 2017.

[8] F. A. de Santos, G. C. V. Iulianelli, and M. I. B. Tavares, "Effect of microcrystalline and nanocrystals cellulose pigments in materials based on PLA matrix," *Polymer Testing*, vol. 61, no. pp. 280-288, 2017.

[9] A. Jacob, "Holland Colours launches bio-derived colorants for personal care packaging & biopolymers; invests in further upgrades," *Additives for Polymers*, vol. 2017, no. 3, pp. 1-2, 2017, doi: 10.1016/S0306-3747(17)30032-5.

[10] T. Hussain, M. Tausif, and M. Ashraf, "A review of progress in the dyeing of eco-friendly aliphatic polyester-based polylactic acid fabrics," *Journal of Cleaner Production*, vol. 108 Part A, no. pp. 476-483, 2015.

[11] N. P. Nirmal, M. S. Rajput, R. G. S. V. Prasad, and M. Ahmad, "Brazilin from Caesalpiniasappan heartwood and its pharmacological activities: A review," *Asian Pacific Journal of Tropical Medicine*, vol. 8, no. 6, pp. 421-430, 2015.

[12] P. Ohama and N. Tumpat, "Textile dyeing with natural dye from Sappan tree (*Caesalpinia sappan* Linn.) extract," *International Journal of Chemical, Molecular, Nuclear, Materials and Metallurgical Engineering*, vol. 8, no. 5, pp. 432-434, 2014.

[13] M. A. Maynez-Rojasa, E. Casanova-González, and J. L. Ruvalcaba-Sil, "Identification of natural red and purple dyes on textiles by fiber-optics reflectance spectroscopy," *Spectrochimica Acta Part A: Molecular and Biomolecular Spectroscopy*, vol. 179, no. pp. 239-250, 2017.

[14] D.-K. Lee, D.-H. Cho, J.-H. Lee, and H. Y. Shin, "Fabrication of nontoxic natural dye from sappan wood," *Korean J. Chem. Eng*, vol. 25, no. 2, pp. 354-358, 2008.

[15] S. Girdthep, J. Sirirak, D. Daranarong, R. Daengngern, and S. Chayabutra, "Physico-chemical characterization of natural lake pigments obtained from *Caesalpinia Sappan* Linn. and their composite films for poly(lactic acid)-based packaging materials," *Dyes and Pigments*, vol. 157, no. pp. 27-39, 2018.

[16] D. Battegazzore, S. Bocchini, and A. Frache, "Crystallization kinetics of poly(lactic acid)-talc biocomposites," *eXPRESS Polymer Letters*, vol. 5, no. 10, pp. 849-858, 2011.

[17] M. Deng, G. Zhang, Y. Zeng, X. Pei, R. Huang, and J. Lin, "Simple process for synthesis of layered sodium silicates using rice husk ash as silica source," *Journal of Alloys and Compounds*, vol. 683, pp. 412-417, 2016.

[18] S. Mor, K. Chhoden, and K. Ravindra, "Application of agro-waste rice husk ash for the removal of

phosphate from the wastewater," *Journal of Cleaner Production*, vol. 129, no. pp. 673-680, 2016.
[19] L. F. C. de Oliveira, H. G. M. Edwards, E. S. Velozoc, and M. Nesbitt, "Vibrational spectroscopic study of brazilin and brazilein, the main constituents of brazilwood from Brazil," *Vibrational Spectroscopy*, vol. 28, no. 2, pp. 243-249, 2002.
[20] T.-H. Liou and C.-C. Yang, "Synthesis and surface characteristics of nanosilica produced from alkali-extracted rice husk ash," *Materials Science and Engineering: B*, vol. 176, no. 7, pp. 521-529, 2011.
[21] C. Drummond, R. McCann, and S. V. Patwardhan, "A feasibility study of the biologically inspired green manufacturing of precipitated silica," *Chemical Engineering Journal*, vol. 244, no. pp. 483-492, 2014.
[22] S. Sankar, N. Kaur, S. Lee, and D. Y. Kim, "Rapid sonochemical synthesis of spherical silica nanoparticles derived from brown rice husk," *Ceramics International*, vol. 44, no. 7, pp. 8720-8724, 2018.
[23] S. Rojtanatanya and T. Pongjanyakul, "Propranolol–magnesium aluminum silicate complex dispersions and particles: Characterization and factors influencing drug release," *International Journal of Pharmaceutics*, vol. 383, no. 1-2, pp. 106-115, 2010.
[24] P. Kumari and Y. Dwivedi, "Investigation of bright red emitting Mn doped aluminum silicate nanophosphor," *Materials Research Bulletin*, vol. 88, no. pp. 266-271, 2017.
[25] B. C. Donose, A. V. Nguyen, G. M. Evans, and Y. Yan, "Effect of aluminium sulphate on interactions between silica surfaces studied by atomic force microscopy," *Water research*, vol. 41, no. pp. 3449-3457, 2007.
[26] A. Dorigato, M. Sebastiani, A. Pegoretti, and L. Fambri, "Effect of silica nanoparticles on the mechanical performances of poly(lactic acid)," *Journal of Polymers and the Environment*, vol. 20, no. 3, pp. 713-725, 2012.
[27] A. Abdulkhani, J. Hosseinzadeh, A. Ashori, S. Dadashi, and Z. Takzare, "Preparation and characterization of modified cellulose nanofibers reinforced polylactic acid nanocomposite," *Polymer Testing*, vol. 35, no. pp. 73-79, 2014.
[28] M. A. Ortenzi, L. Basilissi, H. Farina, G. D. Silvestro, L. Piergiovanni, and E. Mascheroni, "Evaluation of crystallinity and gas barrier properties of films obtained from PLA nanobiocomposites synthesized via 'in situ' polymerization of l-lactide with silane-modified nanosilica and montmorillonite," *European Polymer Journal*, vol. 66, no. pp. 478-491, 2015.
[29] F. R. Beltrán, V. Lorenzo, J. Acosta, M. U. de la Orden, and J. M. Urreagaa, "Effect of simulated mechanical recycling processes on the structure and properties of poly(lactic acid)," *Journal of Environmental Management*, vol. 216, no. pp. 25-31, 2018.
[30] M. C. Divakar, J. V. Susheel, and S. Lakshmidevi, "The analytical and toxicological profiles of the red dye from the heart wood of *Caesalpinia sappan*," *Phcog. Net*, vol. 1, no. 4, pp. 246-250, 2009.
[31] R. Al-Itry, K. Lamnawar, and A. Maazouz, "Improvement of thermal stability, rheological and mechanical properties of PLA, PBAT and their blends by reactive extrusion with functionalized epoxy," *Polymer Degradation and Stability*, vol. 97, no. pp. 1898-1914, 2012.

Pajaera Patanathabutr is a full-time faculty in the position of assistant professor at the Department of Materials Science and Engineering, Faculty of Engineering and Industrial Technology, Silpakorn University, Thailand. She graduated her B.Sc. from Chulalongkorn University, Thailand (1996) and Ph.D. from University of Cambridge, UK (1999). Her research interests are in Natural Dyeing and Biocomposites.

Nattakarn Hongsriphan is a full-time faculty in the position of associate professor at the Department of Materials Science and Engineering, Faculty of Engineering and Industrial Technology, Silpakorn University, Thailand. She graduated her bachelor degree in Chemistry at Chiangmai University, Thailand (1997), and graduated her Doctor of Engineering in Plastics Engineering at the University of Massachusetts Lowell, USA (2003). She is the author of two books (in Thai language) and more than 40 journal articles. Her research interests include polymer blends, polymer biocomposites, and polymer processing.